Proton Nuclear Magnetic Resonance Study of the Molecular and Electronic Structure of the Heme Cavity in *Aplysia* Cyanometmyoglobin†

David H. Peyton,‡ Gerd N. La Mar,*,‡ Usha Pande,‡ Franca Ascoli,§ Kevin M. Smith,‡ Ravindra K. Pandey,‡ Daniel W. Parish,‡ Martino Bolognesi,∥ and Maurizio Brunori⊥,#

Department of Chemistry, University of California, Davis, Davis, California 95616, Department of Experimental Medicine and Biochemical Sciences, University of Rome Tor Vergata, 00173 Rome, Italy, Department of Biochemical Sciences, CNR Center of Molecular Biology, University of Rome La Sapienza, 00185 Rome, Italy, and Section Crystallography, Department of Genetics and Microbiology, University of Pavia, I-27100 Pavia, Italy

Received October 27, 1988; Revised Manuscript Received February 9, 1989

ABSTRACT: The ^{1}H NMR spectrum of the low-spin, cyanide-ligated ferric complex of the myoglobin from the mollusc *Aplysia limacina* has been investigated. All of the resolved resonances from both the hemin and the proximal histidine have been assigned by a combination of isotope labeling, spin decoupling, analysis of differential paramagnetic relaxation, and nuclear Overhauser (NOE) experiments. The pattern of the heme contact shifts is unprecedented for low-spin ferric hemoproteins in exhibiting minimal rhombic asymmetry. This low in-plane asymmetry is correlated with the X-ray-determined orientation of the proximal histidyl imidazole plane relative to the heme and provides an important test case for the interpretation of hyperfine shifts of low-spin ferric hemoproteins. The bonding of the proximal histidine is shown to be similar to that in sperm whale myoglobin and is largely unperturbed by conformational transitions down to pH ~4. The two observed conformational transitions appear to be linked to the titration of the two heme propionate groups, which are suggested to exist in various orientations as a function of both pH and temperature. Heme orientational disorder in the ratio 5:1 was demonstrated by both isotope labeling and NOE experiments. The exchange rate with bulk water of the proximal histidyl labile ring proton is faster in *Aplysia* than in sperm whale myoglobin, consistent with a greater tendency for local unfolding of the heme pocket in the former protein. A similar increased heme pocket lability in *Aplysia* myoglobin has been noted in the rate of heme reorientation [Bellelli, A., Foon, R., Ascoli, F., & Brunori, M. (1987) *Biochem. J. 246*, 787-789].

The monomeric myoglobin (Mb)[1] from the buccal muscle of the mollusc *Aplysia limacina* possesses several interesting properties that distinguish it from the more commonly characterized mammalian Mbs. The sole histidine of the 146 amino acid polypeptide is the proximal F8 ligand (Tentori et al., 1983), and the distal E7 site is occupied by a valine (Bolognesi et al., 1989). The rather open heme pocket and the absence of a distal His in *Aplysia* Mb (Bolognesi et al., 1985) are consistent with a much more rapid oxygen dissociation rate than in sperm whale Mb (Wittenberg et al., 1965). In the oxidized state, the iron(III) is five-coordinate at neutral to low pH (Giacometti et al., 1981a,b), where other Mbs generally bind a water molecule. The protein appears to possess the now common heme orientational heterogeneity, where heme insertion for the two isomers differs by a 180° rotation about the α,γ-meso axis (parts A and B of Figure 1) (La Mar et al., 1983; Lecomte et al., 1985; Pande et al., 1986). Perhaps the most intriguing property of *Aplysia* Mb, however, is its ability to *unfold reversibly* under conditions of thermal, organic agent, or acid denaturation (Brunori et al., 1972; Giacometti et al., 1979; Janes et al., 1987). Thus, this protein is unique among characterized Mbs and provides an important prototype for studying in detail the mechanism of refolding for this class of proteins.

Nuclear magnetic resonance (NMR) is particularly well suited for detailed characterization of the solution molecular/electronic structure of hemoproteins (Morrow & Gurd, 1975; La Mar, 1979; Satterlee, 1986) and can be expected to provide valuable information on the unfolding mechanisms (i.e., local unfolding, intermedaites, conformational transitions induced by the various denaturants). To focus on events in the heme pocket that may accompany various stages of denaturation (i.e., breaking of the axial ligand bond), it is advantageous to investigate paramagnetic forms of hemoproteins where the resonances are likely to be resolved for the residues in the heme pocket and where the spectral parameters are exquisitely sensitive to the detailed folding of the protein (La Mar, 1979; Satterlee, 1986). The initial step in such a study is the detailed characterization of the solution structure of the holoprotein. A high-resolution X-ray structure for *Aplysia* metMb has been reported that allows comparisons with other Mbs (Bolognesi et al., 1985, 1989).

We have shown that NMR spectra of *Aplysia* metMb provide support for the conservation of the five-coordinate structure at neutral pH and establish the existence of a molecular heterogeneity that appears to be related to heme rotational disorder (Pande et al., 1986). The characterization

† This research was supported by grants from the National Institutes of Health [HL-16087 (G.N.L.) and HL-22252 (K.M.S.)], Consiglio Nazionale delle Ricerche [CU 87.00035.04 (F.A.)], and the Ministero della Pubblica Istruzione, Italy (M.B.).

‡ University of California, Davis.
§ University of Rome Tor Vergata.
∥ University of Pavia.
⊥ University of Rome La Sapienza.
Fogarty Scholar-in-Residence, National Institutes of Health (Bethesda).

[1] Abbreviations: Mb, myoglobin; Hb, hemoglobin; metMbCN, cyanometmyoglobin; NMR, nuclear magnetic resonance; ppm, parts per million; DSS, 2,2-dimethyl-2-silapentane-5-sulfonate.

0006-2960/89/0428-4880$01.50/0

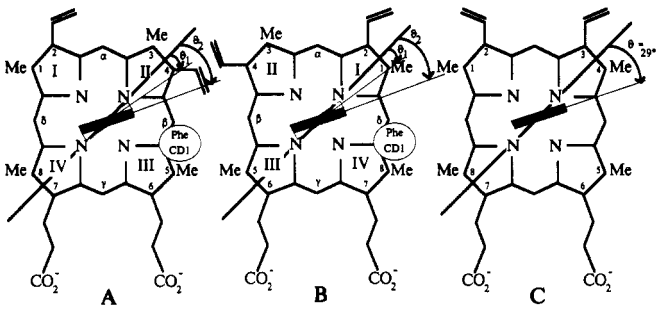

FIGURE 1: Configuration of the heme as viewed from the proximal side in *Aplysia* (Bolognesi et al., 1989) and sperm whale Mb (Kuriyan et al., 1986). (A) Native protohemin as found in the crystal structure; (B) native protohemin reversed by 180° about the α,β-meso axis; (C) symmetric protohemin III reconstituted into the protein; the positions of the 3-CH_3 and 4-vinyl are reversed, leading to symmetry about the α,γ-meso axis. The solid and open rectangles indicate the orientation of the projection of the His F8 imidazole plane, defined by angle θ to the N–Fe–N vector, for *Aplysia* ($\theta_2 \sim 29°$) and sperm whale ($\theta_1 \sim 12°$) Mb, respectively.

of such heme orientational disorder, however, is generally much more directly carried out on the low-spin, six-coordinated cyanide-ligated species (La Mar et al., 1983); Lecomte et al., 1985). In this derivative, the large rhombic anisotropy can impose a large asymmetry in the delocalized spin density distribution and allow the detection of dipolar shifted resonances from amino acid residues that line the heme pocket (Shulman et al., 1971; La Mar, 1979; Satterlee, 1986). The crystal structure suggests that *Aplysia* Mb additionally provides a unique test case for the model on whose basis the ferric, low-spin heme ^{1}H NMR contact shift pattern is interpreted in terms of detailed electronic/molecular structure (Shulman et al., 1971; La Mar, 1978; Traylor & Berzinis, 1980). The major determining factor in this pattern is the angle between the proximal His F8 imidazole plane projection relative to the heme. In most structurally characterized hemoproteins, this projection lies close to one of the two N–Fe–N vectors (for sperm whale MbCO, $\theta \sim 12°$ in Figure 1) (Kuriyan et al., 1986) and is the basis for both ^{1}H NMR detection of heme rotational disorder and determination of the absolute orientation of the heme. In *Aplysia* Mb, however, the His F8 imidazole projection lies closer to a meso–Fe–meso axis (θ determined as $\sim 29°$ in Figure 1) (Bolognesi et al., 1989), for which the heme methyl contact shift asymmetry is predicted to collapse to that observed for a model complex outside the protein matrix (Shulman et al., 1971; La Mar, 1979).

We present herein the detailed assignment of the hyperfine shifted resonances in the ^{1}H NMR spectrum of *Aplysia* metMbCN using a combination of isotope labeling of the heme, analysis of differential iron-induced dipolar relaxation, and the nuclear Overhauser effect (NOE). The resulting hyperfine shift pattern for both the heme and amino acid signals is unprecedented for low-spin ferric hemoproteins and suggests a minimal effective rhombic influence of the folded protein on the heme electronic/magnetic properties. This minimal effective rhombic perturbation, however, is shown not to arise from a weakened interaction between the iron and the proximal histidine, even at pH near acid denaturation.

Experimental Procedures

The native *Aplysia* Mb and the proteins reconstituted with selectively deuterated hemins are the same samples described in detail previously (Pande et al., 1986). The cyanide complexes were prepared by adding 2–5-fold excess of potassium cyanide directly to the met-*Aplysia* solutions. Samples were exchanged into 200 mM NaCl in ^2H_2O or ^1H_2O (10% ^2H_2O was retained for the lock channel) as required, and pH values were adjusted with NaOH (NaO^{2}H) or HCl (^{2}HCl) as needed; pH values were not corrected for the isotope effect. All pH measurements were performed with an Ingold microcombination electrode and a Beckman 3550 pH meter.

^{1}H NMR spectra were collected with Nicolet NT-360 or NT-500 spectrometers operating at 360 and 500 MHz, respectively, with presaturation of the water resonance by a 300-ms decoupler pulse, as required to avoid overfilling the analog-to-digital converter. The 90° pulse width was typically 7 μs (360 MHz) or 11 μs (500 MHz). Spectra were collected with a repetition time of 1.1 s, using quadrature detection with ±6 kHz (360 MHz) or ±10 kHz (500 MHz) bandwidths, and the free induction decay was multiplied by an exponential leading to 5 or 10 Hz line broadening in the transformed spectra. Chemical shifts are referenced to 2,2-dimethyl-2-silapentane-5-sulfonate (DSS) through the residual water signal. Data were processed either with the NMC program supplied with the Nicolet 1280 data system or transferred to a MicroVax II and processed with the program FTNMR supplied by D. Hare. T_1 studies were performed by the usual (composite–180°)–τ–90°–acquire sequence (Levitt, 1982); for ^1H_2O samples, the water resonance was irradiated except during the acquisition. Super-WEFT experiments were simply nonselective T_1 experiments, but with repetition times of 20–200 ms and delay values (τ) of 2–150 ms (Benz et al., 1972).

Nonselective relaxation times were used to estimate the distance of protons to the iron by using (Cutnell et al., 1981)

$$T_{1i}/T_{1j} = r_i^6/r_j^6 \quad (1)$$

where $r_{i(j)}$ is the distance from proton $i(j)$ to the paramagnetic center and $T_{1i(j)}$ is the longitudinal relaxation time from spin $i(j)$. Thus, r_i for a spin can be determined by using $r_j = 6.1$ Å, T_{1j} for the longest relaxing heme methyl, and T_{1i} for spin i.

NOE experiments were performed at 500 MHz by using a repetition rate of 1.5 s and a preirradiation time of 150–300 ms. Typically, 1024 scans were accumulated for each irradiation frequency in the NOE experiments, cycling through the decoupler list after each collection of 64 or 128 scans gained for each irradiation frequency. Saturation-transfer experiments were performed by using the Redfield pulse scheme (Redfield et al., 1975), and on- and off-resonance irradiation of the water was performed for 350 ms prior to excitation and acquisition (Lecomte & La Mar, 1985). As in the NOE experiments, recycling every 64 or 128 scans was employed. The saturation factor, $F = I/I_0$ (I and I_0 being the measured intensity of the exchanging resonance with on-H_2O and off-H_2O irradiation, respectively), was then determined and related to the exchange rate by (Lecomte & La Mar, 1985)

$$\tau^{-1} = \rho(1 - F)/F$$

where ρ is the intrinsic relaxation rate and τ is the lifetime of the proton in the site under investigation. ρ was taken as the T_1 value at a pH where exchange effects with H_2O are negligible ($F = 1.0$). Although the selective T_1 is required, the T_1 of the resonance of interest (a_1*) is predominantly influenced by paramagnetism, so that selective and nonselective T_1s are essentially the same (Lecomte & La Mar, 1985, 1986).

Results

Spectra Analysis of Native Protein. The resolved portions of the 500-MHz ^{1}H NMR spectrum of *Aplysia* metMbCN in ^2H_2O, pH 9.2, are shown in Figure 2A. As previously

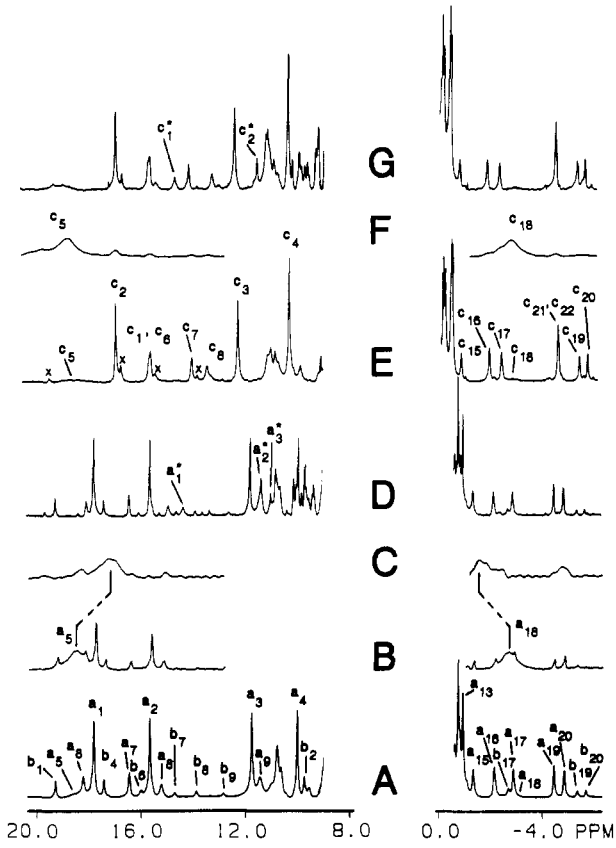

FIGURE 2: Hyperfine-shifted portions of the 500-MHz ^1H NMR spectra of *Aplysia* metMbCN at 25 °C. (A) Native protein in ^2H_2O at pH 9.24; the peaks for the major and minor isomers are labeled a_i and b_i, respectively. (B) Native protein super-WEFT spectrum in ^2H_2O at pH 9.24. (C) Native protein super-WEFT spectrum in ^2H_2O at pH 4.02. (D) Native protein in ^1H_2O at pH 9.33. (E) Protohemin-III reconstituted *Aplysia* metMbCN in ^2H_2O at pH 8.91; peaks are labeled c_i. (F) Protohemin-III-reconstituted protein super-WEFT spectrum in ^2H_2O at pH 8.91. (G) Protohemin-III-reconstituted protein in ^1H_2O at pH 9.35.

observed for high-spin metMb (Pande ett al., 1986), the spectrum reflects two species for which peaks a_1–a_4, a_{13}, and b_1–b_3 arise from methyls from the major (~80%) and minor (~20%) isomer, respectively. The resolved single-proton peaks for the major isomer are labeled a_5–a_9 and a_{15}–a_{20}; a composite of peaks (approximately three protons total) occurs at 10.7 ppm. The very broad single proton peaks a_5 and a_{18} are not readily detected in a normal spectrum, but are clearly observed in a super-WEFT spectrum (Figure 2B) that emphasizes that rapidly relaxing peaks. Peak areas at intermediate delay times establish that both a_5 and a_{18} arise from single protons with $T_1 \lesssim 2$ ms. The peaks b_6–b_9, b_{17}, b_{19}, and b_{20} have intensities consistent with their arising from single protons from the minor isomer.

Comparison of the trace in ^2H_2O (Figure 2A) with that in ^1H_2O (Figure 2C) reveals several labile single-proton resonances, a_1*, a_2*, and a_3*, of which only a_1* exhibits strong paramagnetic shift and relaxation effects. A nonselective T_1 determination in ^1H_2O yielded the values given in Table I; only the major component peaks are listed. A study of the influence of temperature on the observed shifts at pH 9.2 (far from any p*K*) yielded linear plots of shift versus reciprocal temperature (Curie plot) (Jesson, 1973), but with apparent intercepts at $T^{-1} = 0$, disparate with expectation from known diamagnetic origins: representative Curie plots for the native protein are shown in Figure 3, and representative intercepts at $T^{-1} = 0$ are included in Table I.

Table I: ^1H NMR Spectral Parameters for *Aplysia* MetMbCN

resonance label[a]	assignment	chemical shift[a,b]	T_1[c]	diamagnetic intercept[a,d]
	Native Cyanomet *Aplysia* Mb			
a_1 (b_1)	3-CH_3	17.81 (19.34)	140	0.5 (0.5)
a_2 (b_2)	5-CH_3	15.66 (9.64)	150	11.7 (15.6)
a_3	1-CH_3	11.78	170	6.2
a_4 (b_4)	8-CH_3	9.91 (17.44)	267	14.7 (9.2)
a_5	His 95 ring CH	18.6	~3	
a_6	6-H_α	18.14	149	−4.9
a_7	2-H_α	16.47	185	7.0
a_8	6-H_α	15.15	143	−22.0
a_{10}	6-H_β	1.57		
a_{15}	6-H_β	−1.35		2.9
a_{16}	7-H_β	−2.21	176	6.0
a_{17}	7-H_β	−2.89	155	9.8
a_{18}	His 95 ring CH	−2.6	~3	
a_{19}	2-$H_{\beta c}$	−4.51	158	9.2
a_{20}	2-$H_{\beta t}$	−4.89	199	11.6
a_1*	His 95 N_3H	14.32	33	
	Protohemin-III-Reconstituted Cyanomet *Aplysia* Mb			
c_1		15.37		−1.7
c_2	5-CH_3	16.68		8.9
c_3	1-CH_3	11.99		6.2
c_4	8-CH_3	10.05		15.1
c_5	His 95 C_4H	18.5		
c_6		15.37		6.9
c_7		13.78		13.0
c_8		13.15		−9.5
c_{15}		−1.11		3.2
c_{16}		−2.18		6.2
c_{17}		−2.63		9.6
c_{18}		−2.7		
c_{19}		−5.60		7.4
c_{20}		−5.92		10.9
c_{21}		−4.80		9.6
c_{22}		−4.80		9.6
c_1*	His 95 N_3H	14.4		

[a] 25 °C. For major isomer, a_i; methyl peaks for minor isomer, b_i, given in parentheses. [b] 25 °C. Native protein, pH 8.52; pH 8.9 for protohemin-III-reconstituted protein. [c] 25 °C. pH 7.7. [d] 25 °C. Native protein, pH 8.06; pH 8.9 for protohemin-III-reconstituted protein.

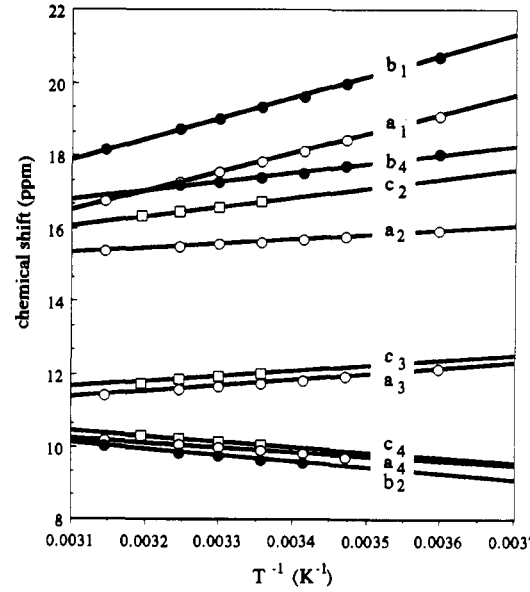

FIGURE 3: Plot of chemical shift vs reciprocal temperature (Curie plot) for indicated resonances (all resolved methyls) in native *Aplysia* metMbCN [major isomer peaks a_i (open circles); minor isomer, b_i (solid circles)] and in protohemin-III-reconstituted *Aplysia* metMbCN (peaks c_i, open squares), in ^2H_2O and pH 9.24. Intercepts at $T^{-1} = 0$ are given in Table I.

The influence of solution pH on observed shifts in the range 3.7–9.5 at 25 °C in ^2H_2O (and in ^1H_2O for peak a_1*) is illustrated in Figure 4. The data are qualitatively consistent

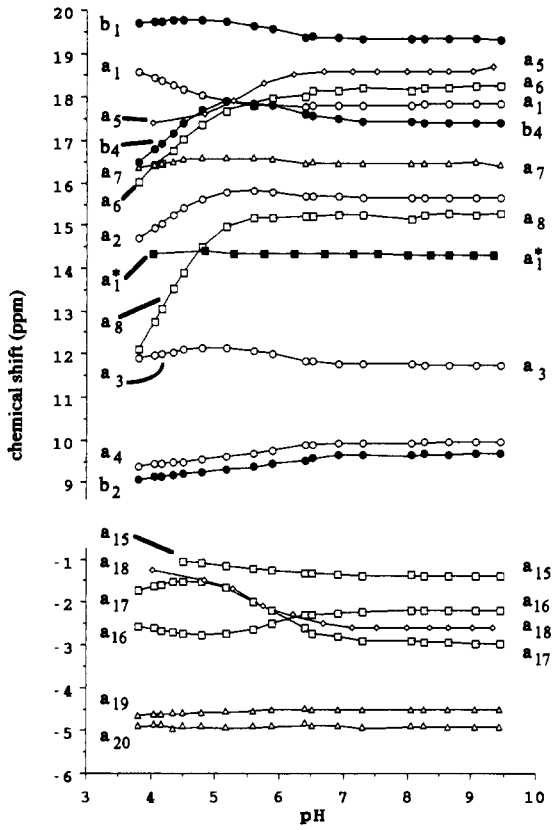

FIGURE 4: pH dependence of resolved resonances of the ^1H NMR spectrum of *Aplysia* metMbCN. The lines are intended only as a guide to the eye in following the titration of each resonance. Symbols: Methyl protons (circles); vinyl protons (triangles); propionate protons (squares); His F8 protons (diamonds). Open symbols are from the major form, a_i, and solid symbols are from the minor form, b_i (methyls only).

with the presence of two p*K*s at $\lesssim$4.2 and $\sim$6. Below pH 3.7 precipitation occurs at the concentrations needed to determine the holoprotein structure. It is noted that labile proton signal a_1* and the two broad single-proton peaks a_5 and a_{18} neither lose intensity, exhibit line narrowing (i.e., decrease in paramagnetic relaxation) (see Figure 2C), nor display a large shift change upon lowering the pH to 3.7 (Figure 4).

Protein Reconstituted with Symmetric Hemin. The 500-MHz ^1H NMR traces of protohemin-III-reconstituted (Figure 1C) *Aplysia* metMbCN in ^2H_2O and ^1H_2O are shown in parts E and G, respectively, of Figure 2. Obvious methyl peaks are labeled c_2, c_3, and C_4, single-proton peaks, c_i, and labile protons c_1* and c_2*. A super-WEFT trace that emphasizes the rapidly relaxing, broad single-proton peaks c_5 and c_{18} is shown in Figure 2F. The spectrum of this protein (Figure 2E) closely resembles that of the native protein (Figure 2A) except that there is only one set of peaks, a missing low-field methyl, and the presence of additional single-proton peaks c_1, c_{21}, and c_{22} (compare shifts in Table I). The very small peaks marked × are due to an impurity that can be removed by exhaustive purification (Pande et al., 1986).

Isotope Labeling of Hemin. The 360-MHz ^1H NMR traces of *Aplysia* metMbCN containing protohemin deuterated solely at 8-methyl (Figure 5B), at both 1- and 3-methyls (Figure 5C), and at both 1- and 5-methyls (Figure 5D) unequivocally establish the major isomer methyl assignments a_1 = 3-CH_3, a_2 = 5-cH_3, a_3 = 1-CH_3, and a_4 = 8-CH_3. Moreover, the only intensity changes for minor isomer methyls identify b_1 = 3-CH_3, b_4 = 8-CH_3, and b_2 = 5-CH_3 and dictate that the minor isomer 1-CH_3 signal must resonate in the intense diamagnetic envelope, 0–9 ppm.

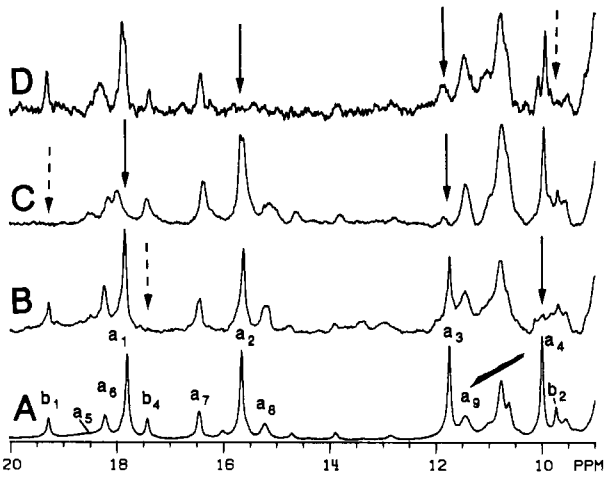

FIGURE 5: Assignment of downfield-shifted heme methyl resonances in *Aplysia* metMbCN in ^2H_2O at 25 °C based on methyl deuteration. (A) Native at pH 9.34; (B) reconstituted with 8-methyl deuterated hemin, pH 9.7; (C) reconstituted with 1- and 3-methyl deuterated hemin, pH 9.6; (D) reconstituted with 1- and 5-methyl deuterated hemin, pH 9.6. Arrows indicate attenuated resonances due to selective deuteration of the major form (solid arrows) and minor form (dashed arrows). These demonstrate the following assignments: (from the major form) a_1, 3-CH_3; a_2, 5-CH_3; a_3, 1-CH_3; and a_4, 8-CH_3; (from the minor form) b_1, 3-CH_3; b_2, 5-CH_3; and b_4, 8-CH_3.

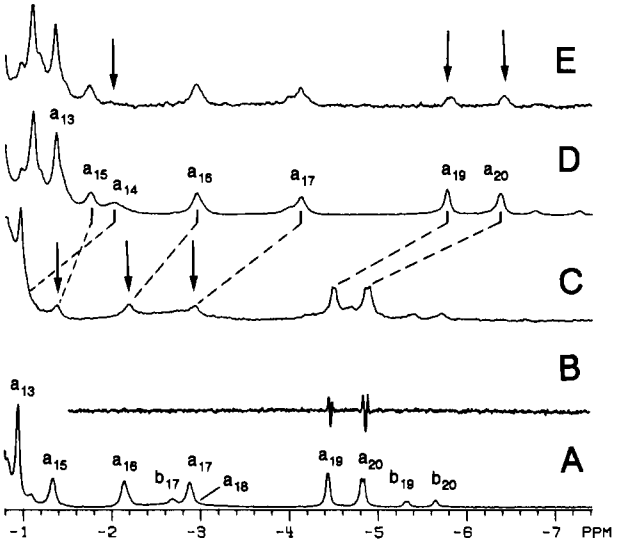

FIGURE 6: Partial assignment of upfield-shifted heme resonances in *Aplysia* metMbCN in ^2H_2O. (A) 500-MHz spectrum at 25 °C and pH 9.24; (B) 360-MHz difference spectrum generated by selective gated irradiation on and off a_7 during acquisition at 25 °C, pH 9.24; (C) 500-MHz spectrum of 1- and 3-methyl deuterated hemin reconstituted protein at 25 °C and pH 9.26, which shows partial deuteration at the β-propionates; (D) 500-MHz spectrum at 0 °C and pH 9.24; (E) spectrum of $^2H_4$-meso-protohemin IX reconstituted protein at 0 °C and pH 9.08, which shows selective deuteration at a meso proton (a_{14}) and partial deuteration of vinyl H_βs a_{19} and a_{20}.

On-acquisition irradiation of a_7 collapses multiplet structure for peaks a_{19} and a_{20} (Figure 6B) with the characteristic $J \sim$ 16 Hz for a_{20}, identifying a_7, a_{19}, and a_{20} as H_α, $H_{\beta c}$, and $H_{\beta t}$ of a single vinyl group (La Mar et al., 1978). The sample perdeuterated at the 1- and 3-methyls (Figure 5C) also has $\sim$80% deuteration of the β-propionate positions (Pande et al., 1986; Lecomte et al., 1987); the reduced intensity of peaks a_{15}, a_{16}, and a_{17} (Figure 6C) thus dictates that their origins are three of the four propionate β-CHs. When the temperature is lowered to 0 °C, one additional single proton peak becomes resolved in the upfield window, a_{14} (Figure 6D), which disappears in a sample containing hemin perdeuterated at all four meso positions (Figure 6E) (Pande et al., 1986); note, this

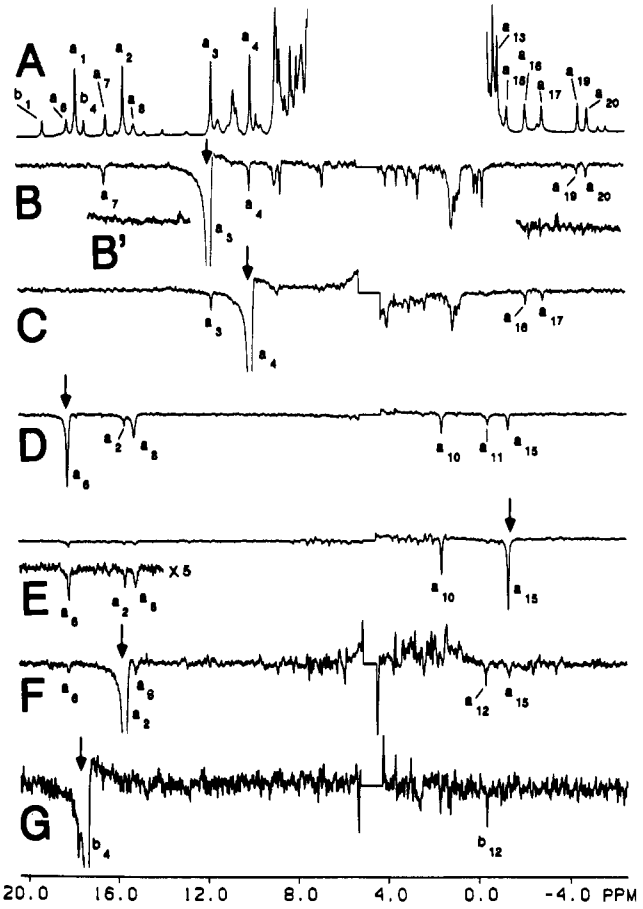

FIGURE 7: 500-MHz NOE difference spectra of *Aplysia* metMbCN in ^2H_2O at 25 °C. (A) Reference spectrum. (B) NOE difference spectrum from irradiating a_3 (1-CH_3). Note NOEs to a_4 (8-CH_3), a_{19} and a_{20} (2-vinyl H_βs), and a_7 (2-vinyl H_α). This is confirmed by the absence of NOEs to the vinyl protons a_7, a_{19}, and a_{20} when a_1 (3-CH_3) is saturated as shown in inset B'. (C) NOE difference spectrum upon irradiating a_4 (8-CH_3); note NOEs to a_{16} and a_{17} (7-propionate H_βs). (D) NOE difference spectrum upon irradiating a_6 (6-H_α). Note NOEs to a_2 (5-CH_3), a_8 (6-H_α; geminal partner to a_6), and a_{10} and a_{15} (6-H_βs). (E) NOE difference spectrum upon irradiating a_{15} (6-H_β). Note NOEs to a_2 and a_6 (6-H_αs), a_2 (5-CH_3), and a_{10} (geminal 6-H_β). (F) NOE difference spectrum upon irradiating a_2 (5-CH_3). Note NOEs to a_2 and a_8 (6-H_αs) and a_{15} (6-H_β). Note also the presence of amino acid peak a_{12}, which is entirely absent in traces B and C. (G) NOE difference spectrum upon irradiating b_4 (8-CH_3) from the minor form. Note the similarity to trace F, especially the presence of b_{12}, which is absent in trace C. Thus, pairwise exchange between a_2 (5-CH_3) and b_4 (8-CH_3) is demonstrated.

sample also has ~50% deuteration of vinyl H_βs, leading to reduced intensity for a_{19} and a_{20} as well.

NOE Studies. On-resonance saturation of a_3 (1-CH_3) yields small NOEs to both a_7 (H_α) and a_{19} and a_{20} (H_βs) (Figure 7B), while saturation of a_1 (3-CH_3) fails to influence a_7, a_{19}, or a_{20} (Figure 7B'); hence, the peaks a_7, a_{19}, and a_{20} originate from the 2-vinyl rather than the 4-vinyl group (Peyton et al., 1988). A small NOE from a_3 (1-CH_3) to a_4 (8-CH_3) is consistent with observations for the same two peaks in sperm whale metMbCN (La Mar et al., 1986). Saturation of a_4 produces the expected NOE to a_3 (8-CH_3 → 1-CH_3) and NOEs to propionate H_β peaks a_{16} and a_{17}, which are therefore assigned to the 7-propionate side chain (Figure 7C). This is confirmed by a strong (>35%) NOE between a_{16} and a_{17}, establishing them as geminal partners (not shown). Saturation of a_6 gives a small NOE to a_2 (5-CH_3) and a large (~35%) NOE to a_8 (Figure 7D). The large NOE between a_2 and a_8 establishes them as geminal partners of a methylene group. The NOE to a_{15} (assigned to a propionate H_β above), as well as to a_2 (5-CH_3), dictates that a_2 and a_8 originate from the 6-propionate α-CH_2. Saturation of a_{15} (Figure 7E) not only yields the expected reciprocal NOEs to a_2, a_8 (6-α-cH_2), and a_2 (5-CH_3) but also yields a ~50% NOE to a_{13} at 2.8 ppm, identifying a_{10} and a_{15} as the propionate 6-β-CH_2. Saturation of a_2 (5-CH_3) yields the NOE difference trace shown in Figure 7F that, in addition to exhibiting the expected NOEs to 6-H_α peak a_6,a_8 and 6-H_β peak a_{15}, displays a prominent NOE to an amino acid peak near 0 ppm that we label a_{12}. Irradiating the meso proton signal a_{14} at 0 °C produces an NOE to a_6, 6-H_α (not shown); hence, a_{14} must arise from the hemin γ-meso-H. Saturation of exchangeable peak a_1* in the native protein leads to an NOE in the other labile proton a_2* (not shown).

Discussion

Resonance Assignment. The combination of isotope labeling and NOEs for the native protein locate and assign for the major isomer 14 of the 22 heme signals and show that the remaining 8, 3 meso-Hs, 3 4-vinyl Hs, and the 2 7-α-CH, resonate in the diamagnetic envelope.

The ^1H NMR spectrum of protohemin III–metMbCN exhibits only three low-field resolved methyl peaks, c_2, c_3, and c_4. Of these, the shifts for c_3 and c_4 are essentially the same as for the native protein peaks a_3 and a_4 and here can be attributed to 1-CH_3 and 8-CH_3, respectively. Methyl c_2 has a shift midway between a_1 and a_2, but is more likely to arise from 5-CH_3; the hyperfine shift for 4-vinyl in the native protein is very small, so we can expect that a 4-CH_3 should be similarly located in the diamagnetic envelope. This assignment of c_2 to 5-CH_3 is supported by variable-temperature data (see below). Also in agreement with this we observe three new single-proton resonances, one downfield (c_1) and two upfield (c_{21}, c_{22}) peaks (degenerate at 25 °C), which should arise from the 3-vinyl H_α and the H_βs and reflect the large spin density at the 3-position relative to the 4-position found in the native protein.

For both the native and protohemin-III-reconstituted Mb complexes, labile single-proton peaks a_1* and c_1* are assigned to the ring NH in the proximal His F8. The most direct support for this is its short relaxation time, ~33 ms, which dictates that it is ~5 Å from the iron via eq 1 (Cutnell et al., 1981). The crystal structure of *Aplysia* metMb reveals only one exchangeable proton less than 7 Å from the metal, namely, the His F8 ring $N_\delta H$ (Bolognesi et al., 1985). Further support is provided by the mechanism of exchange of a_1* with both solvents (see below). The two broad peaks a_5 and a_{18} (and c_5 and c_{18}) exhibit $T_1 \lesssim 3$ ms and hence must be located <4 Å from the iron. Both the short distances and the characteristic low- and high-field shifts assign these two resonances to $C_\delta H$ and $C_\epsilon H$ of the proximal His F8 (La Mar, 1979; La Mar et al., 1982). Similar peaks were observed in sperm whale metMbCN and uniquely assigned by NOEs (Emerson, 1988). The NOE from a_1* to a_2* argues for a_2* (and c_2*) arising from the peptide NH of His F8, again as found in sperm whale metMbCN (Lecomte & La Mar, 1986).

Conformational Transitions. The pH dependence of the shifts (Figure 4) indicates a transition with pK ~ 6 that slightly perturbs the shifts, and another transition with much more dramatic influence on shifts is observed with p$K \lesssim 4$. The pK ~ 6 transition most strongly perturbs the shifts of 7-H_β peaks a_{10} and a_{17} and suggests that it may involve the titration of the 7-propionate group. The low pH transition most strongly influences the shifts of the 6-H_α peaks a_2 and a_8 and the 5-CH_3 peak a_2, indicating that the titration of the

6-propionate may be involved. It is noted, however, that we observe no evidence for global unfolding or denaturation down to pH 3.7; most importantly, neither of the broad peaks a_5 or a_{18} nor the labile proton peak a_1* exhibits significant change in shift or line width down to pH 3.7 (Figures 2B,C and 4), which indicates that the iron remains six-coordinated down to pH 3.7.

Electronic/Magnetic In-Plane Asymmetry. The most prominent change observed when a low-spin hemin is incorporated into a protein matrix is that, while the mean in the four heme methyl contact shifts remains essentially unchanged, the spread in these shifts is greatly increased and reflects the inherent rhombic asymmetry of the protein contacts (Shulman et al., 1971; La Mar, 1979; Traylor & Berzinis, 1980). Thus, the ~3 ppm spread in the methyls in biscyanohemin (La Mar et al., 1978b) increases to 24 ppm (Mayer et al., 1974; La Mar et al., 1983, 1986) upon incorporation into the pocket of sperm whale metMbCN. The dramatic spread of the methyl shifts is characteristic of every structurally characterized low-spin ferric heme protein, ranging over cytochromes (Keller & Wüthrich, 1980), peroxidases (Thanabal et al., 1987), myoglobins (Mayer et al., 1974; La Mar et al., 1986), and hemoglobins (La Mar et al., 1980a; La Mar, 1987). Moreover, in these proteins, the origin and the rhombic perturbations could be traced to the dominant axial ligand bonding: the orientation of the coordinated His imidazole plane in cyanide-ligated Mbs (Shulman et al., 1971; Mayer et al., 1974), Hbs (La Mar et al., 1987), and peroxidases (Satterlee et al., 1983) or the chirality of the axial methionine in cytochromes *c* (Senn et al., 1980).

The hyperfine shift pattern for the heme substituents in *Aplysia* metMbCN has both close similarities and dramatic differences when compared to that of related hemoproteins. On the one hand, the shifts are typically largely π contact in origin (La Mar & Walker (Jensen), 1987; La Mar, 1979), as witnessed by shift direction (low-field methyls, vinyl H_α, upfield vinyl H_βs). Even the mean of the four heme methyl shifts (~14 ppm) is in line with other Mbs. On the other hand, the four methyl shifts are all very similar and not too different from that of the free prosthetic group with two bound cyanides (La Mar et al., 1978b).

The remarkable effective axial electronic symmetry observed by ^{1}H NMR in *Aplysia* metMbCN relative to that in the other proteins, in particular sperm whale metMbCN (Mayer et al., 1974; La Mar et al., 1986), is consistent with expectations that the methyl shift spread would be minimal when the His F8 imidazole projection is coincident with a meso–Fe–meso axis (Shulman et al., 1971; Traylor & Berzinis, 1980). The fact that the spread of the heme methyl contact shifts is not as small as in a model complex outside a protein matrix is probably due to the fact that θ in Figure 1A,B is not 45° and to the presence of other minor determinants in the effective rhombic perturbations, such as the tilt of the bound cyanide (Lecomte & La Mar, 1987). An additional potential effect on the rhombic asymmetry that may be operating in *Aplysia* Mb is a weakened axial interaction with His F8.

The reduced effective asymmetry in *Aplysia* Mb is also reflected in magnetic properties. Noncoordinated amino acid residues exhibit only dipolar shifts that directly reflect magnetic anisotropy, and for sperm whale metMbCN, the contributions from axial and rhombic magnetic anisotropy are substantial (Ramaprasad et al., 1984; Emerson et al., 1988), leading to a spread of amino acid dipolar shifts of ~25 ppm (15 ppm low field to −9 ppm high field). Of the resolved resonances that do not arise from the heme or His F8, the furthest low-field and high-field amino acid signals in *Aplysia* metMbCN are at 11.5 ppm and methyl a_{13} at −0.95 ppm, for a spread of only 12.5 ppm.

Axial Ligand Bonding. It has been suggested that the propensity for breaking the axial His–iron bond at acidic pH is greater in *Aplysia* than in sperm whale Mb (Ascenzi et al., 1984; Brunori et al., 1986). Hence, an overall weaker axial bonding to the imidazole for native *Aplysia* Mb could account, in part, for the decreased rhombic perturbation of the protein. However, it is noted that the His F8 ring $C_\delta H, C_\epsilon H$ (peaks a_5 and a_{18}), hyperfine shifts, and line widths (as well as T_1s) are essentially the same as in sperm whale metMbCN (La Mar et al., 1982; Emerson, 1988). Only the ring $N_\delta H$ (a_1*) shift in *Aplysia* metMbCN is smaller (~15 ppm) than in the sperm whale protein (22 ppm) (Cutnell et al., 1981). The X-ray data confirm similar Fe–His F8 bonding with Fe–N_ϵ distances of 2.05 and 2.13 Å for *Aplysia* and sperm whale Mb, respectively (Bolognesi et al., 1989). More importantly, however, we note that upon lowering the pH to 3.7, the shift and line width of $N_\delta H$ (a_1*) and the line width of $C_\delta H$, $C_\epsilon H$ (peaks a_5 and a_{18}) remain invariant; only the shifts for the latter two protons change slightly (see Figures 2B,C and 4). Hence, we find no evidence for significant differences in the strength of the iron–His F8 bonding between *Aplysia* and sperm whale Mb, and we conclude that the low pH transition does not involve a significant perturbation on the iron–his F8 bonding. Therefore, the spectral changes reported by Ascenzi et al. (1984) are more likely to arise from the protonation of carboxylate, possibly one of the heme propionates.

Internal Averaging of Rhombic Asymmetry. The variable-temperature NMR data provide some evidence that the observed spectral parameters may result, in part, from the averaging over two (or more) alternate structures. Thus, the intercepts at $T^{-1} = 0$ for Curie plots (Figure 3) of heme methyls are generally close to the diamagnetic positions, particularly for the strongly shifted methyls (La Mar, 1979; Satterlee, 1986). As shown in Figure 3 and Table I, however, all four methyls exhibit unusual intercepts. Particularly prominent is the ~12 ppm intercept for a a_2 (5-CH_3). Also noteworthy are the very large upfield intercepts for both 6-α-CHs (a_6, a_8). Since the mean methyl shift does not increase with temperature, a low-spin ⇌ high-spin equilibrium can be ruled out (La Mar et al., 1980b, 1983). In fact, the highly selective deviation from normal Curie behavior (intercept too far upfield for 3-CH_3 and 6-α-CH_2, too far downfield for 1-CH_3, 5-CH_3, and 8-CH_3) suggests dynamic averaging over one or more structures with somewhat different contact shift patterns, where the populations change slightly with temperature.

The X-ray structure of *Aplysia* metMb (Bolognesi et al., 1985, 1989) provides some clues as to the possible origins for conformational heterogeneity which is averaged on the NMR time scale. In contrast to sperm whale Mb (Takano, 1977; Kuriyan et al., 1986), the propionate groups do not appear to participate in specific salt bridges and, in fact, are found either disordered (7-propionate) or with unusually large thermal motions (6-propionate). The appearance of only a single set of propionate ^{1}H NMR resonance for each side chain dictates that these motions be fast on the NMR time scale (Sandström, 1982). The fact that the most prominent deviation from Curie behavior is observed for the 6-propionate α-CH signals, a_2 and a_8, lends support to the conclusion that the propionates can adopt various orientations that can rapidly interconvert. Hence, nonequivalent propionate orientations likely provide a minor influence on the contact shift pattern.

Heme Rotational Disorder. The minimal effective rhombic perturbation of the protein on the heme electronic/magnetic properties eliminates the simplest qualitative tool (La Mar, 1979) for characterizing the existence of the two heme orientations depicted in parts A and B of Figure 1. Thus, in the other low-spin ferric hemoprotein studies to date (La Mar, 1979; Satterlee, 1986), the spread of the heme methyl shift is large, and the two heme orientations lead to a clear interchange between the environments of 5-CH_3 and 8-CH_3 (and between 1-CH_3 and 3-CH_3) in the alternate forms (La Mar et al., 1980a, 1983). The interchange of 5-CH_3 and 8-CH_3 environments is observed in *Aplysia* metMbCN, i.e., 5-CH_3 at 16 ppm (a_2) and 8-CH_3 at ~10 ppm (a_4) for the major isomers and 8-CH_3 at ~17 ppm (b_4) and 5-CH_3 at ~10 ppm (b_2) for the minor isomer. On the other hand, the 3-CH_3 is downfield of the 1-CH_3 peak for both isomers. Thus, both the interchange of the 5-CH_3 and 8-CH_3 environments in the two isomers and the appearance of a single set of resonances for the protein reconstituted with the symmetric protohemin III (Figure 2E) are consistent with heme disorder as the origin of the molecular heterogeneity that gives rise to the two sets of peaks a_i and b_i.

The NOE patterns from heme methyls to the protein matrix, however, provide additional quantitative information on the physical origin of the heterogeneity (Peyton et al., 1988). For the major isomer, the NOE to a single upfield-shifted amino acid peak (a_{12}) from 5-CH_3 (a_2) (Figure 7F) is contrasted with the observation of several strong NOEs from 8-CH_3 (Figure 7C) to amino acid signals near 2 ppm. This difference in NOE patterns when 8-CH_3 and 5-CH_3 are irradiated reflects the different protein environments of the two methyls and can be used to confirm the origin of two sets of peaks a_i and b_i as heme orientational disorder. Thus, saturating the 8-CH_3 (peak b_4) of the minor isomer (Figure 7G) yields the NOE near 0 ppm (peak b_{12}) as seen for 5-CH_3 (a_2) rather than NOEs near 2 ppm for 8-CH_3 (a_4) of the major isomer. Thus, 8-CH_3 and 5-CH_3 must exchange protein environments in the a_i and b_i isomer, as described by parts A and B of Figure 1.

It may be noted that the assignment of the three methyl peaks c_2, c_3, and c_4 to 5-CH_3, 1-CH_2, and 8-CH_3 in protohemin III–metMbCN is also supported by the observation of very similar non-Curie behavior as the clearly identified peaks in the native protein (Figure 3, Table I).

Heme Pocket Dynamics. The labile proton peak a_1* that is assigned to the His F8 ring $N_\delta H$ exhibits unit proton intensity at pH values below 8, but gradually loses intensity and broadens as the pH is raised to 9.5. Redfield-type NMR spectra (Redfield et al., 1975) with and without saturating the bulk water resonance (not shown) reveal saturation transfer from bulk solvent that is consistent with the dominant base-catalyzed exchange mechanism for the iron-bound imidazole previously characterized for a variety of hemoproteins. The saturation factor of 0.5 at pH 8.8, together with a relaxation rate of 30 s^{-1} (Table I) in the absence of exchange yields an exchange rate of 3×10^2 s^{-1} at 25 °C, which is comparable to that observed at the same pH in sperm whale metMbCN at 40 °C (Cutnell et al., 1981; Lecomte & La Mar, 1985). This increase in exchange rate in *Aplysia* relative to sperm whale Mb suggests that local unfolding of the heme pocket occurs more readily in *Aplysia* than in sperm whale Mb. This notion is consistent with the previous observations that the rate of interconversion between the two heme rotational isomers, as determined by CD spectroscopy, has been found to be ~10 times faster in *Aplysia* than in sperm whale Mb (Bellelli et al., 1987).

What is surprising is the absence of any saturation transfer from bulk solvent for the His F8 $N_\delta H$ signal a_1* below pH 4. Since any dissociation in the iron–His bond would provide a highly efficient acid-catalyzed exchange mechanism for the $N_\delta H$, the slow exchange (<30 s^{-1} at pH 4) also supports the maintenance of an intact non-His-F8 bond to very low pH values.

Lowering the pH below 3.7 invariably leads to precipitation of protein at the concentrations (~1–2 mM) considered optimal for the present NMR studies directed at resonance assignment. When the pH is raised above 4, transient spectral features appear that may originate in refolding intermediates. Studies of this process at much lower protein concentration are planned.

ACKNOWLEDGMENTS

We are indebted to J. T. J. Lecomte and V. Thanabal for valuable discussions.

Registry No. L-His, 71-00-1; heme, 14875-96-8.

REFERENCES

Ascenzi, P., Condo, S. G., Bellelli, A., Barra, D., Bannister, W. H., Giardina, B., & Brunori, M. (1984) *Biochim. Biophys. Acta 788*, 281–289.

Bellelli, A., Foon, R., Ascoli, F., & Brunori, M. (1987) *Biochem. J. 246*, 787–789.

Benz, F. W., Feeney, J., & Roberts, G. C. K. (1972) *J. Magn. Reson. 8*, 114–121.

Bolognesi, M., Coda, A., Gatti, G., Ascenzi, P., & Brunori, M. (1985) *J. Mol. Biol. 183*, 113–115.

Bolognesi, M., Onesti, S., Gatti, G., Coda, A., Ascenzi, P., & Brunori, M. (1989) *J. Mol. Biol.* (in press).

Brunori, M., Giacometti, G. M., Antonini, E., & Wyman, J. (1972) *J. Mol. Biol. 63*, 139–152.

Cutnell, J. D., La Mar, G. N., & Kong, S. B. (1981) *J. Am. Chem. Soc. 103*, 3567–3572.

Emerson, S. D. (1989) Ph.D. Thesis, University of California, Davis.

Emerson, S. D., Lecomte, J. T. J., & La Mar, G. N. (1988) *J. Am. Chem. Soc. 110*, 4176–4182.

Giacometti, G. M., Antonini, E., & Brunori, M. (1979) *Biophys. Chem. 10*, 119–127.

Giacometti, G. M., Ascenzi, P., Bolognesi, M., & Brunori, M. (1981a) *J. Mol. Biol. 146*, 363–374.

Giacometti, G. M., Ascenzi, P., Brunori, M., Riagatti, G., Giacometti, G., & Bolognesi, M. (1981b) *J. Mol. Biol. 151*, 315–319.

Janes, S. M., Holtom, G., Ascenzi, P., Brunori, M., & Hochstrasser, R. M. (1987) *Biophys. J. 51*, 653–660.

Jesson, J. P. (1973) in *NMR of Paramagnetic Molecules* (La Mar, G. N., Horrocks, W. D., Jr., & Holm, R. H., Eds.) pp 1–51, Academic Press, New York.

Keller, R. M., & Wüthrich, K. (1981) *Biological Magnetic Resonance* (Berliner, L. J., & Reuben, J., Eds.) pp 1–52, Plenum Press, New York.

La Mar, G. N. (1979) in *Biological Application of Magnetic Resonance* (Shulman, R. G., Ed.) pp 305–343, Academic Press, New York.

La Mar, G. N., & Walker (Jensen), F. A. (1973) in *The Porphyrins* (Dolphin, D., Ed.) Vol. IVB, pp 61–157, Academic Press, New York.

La Mar, G. N., Overkamp, M., Sick, H., & Gersonde, K. (1978a) *Biochemistry 17*, 352–361.

La Mar, G. N., Viscio, D. B., Smith, K. M., Caughey, W. S., & Smith, M. L. (1978b) *J. Am. Chem. Soc. 100*, 8085–8092.

La Mar, G. N., Budd, D. L., & Smith, K. M. (1980a) *Biochim. Biophys. Acta 627*, 210–218.
La Mar, G. N., Smith, K. M., Gersonde, K., Sick, H., & Overkamp, M. (1980b) *J. Biol. Chem. 255*, 66–70.
La Mar, G. N., de Ropp, J. S., Chacko, V. P., Satterlee, J. D., & Erman, J. E. (1982) *Biochim. Biophys. Acta 708*, 317–325.
La Mar, G. N., Davis, H. L., Parish, D. W., & Smith, K. W. (1983) *J. Mol. Biol. 168*, 887–896.
La Mar, G. N., Emerson, S. D., Lecomte, J. T. J., Pande, U., Smith, K. M., Craig, G. W., & Kehres, L. A. (1986) *J. Am. Chem. Soc. 108*, 5568–5573.
Lecomte, J. T. J., & La Mar, G. N. (1985) *Biochemistry 24*, 7388–7395.
Lecomte, J. T. J., & La Mar, G. N. (1986) *Biophys. J. 13*, 373–381.
Lecomte, J. T. J., & La Mar, G. N. (1987) *J. Am. Chem. Soc. 109*, 7219–7220.
Lecomte, J. T. J., Johnson, R. D., & La Mar, G. N. (1985) *Biochim. Biophys. Acta 829*, 268–274.
Lecomte, J. T. J., La Mar, G. N., Smit, J. D. G., Winterhalter, K. H., Smith, K. M., Langry, K. C., & Leung, H.-K. (1987) *J. Mol. Biol. 197*, 101–110.
Levitt, M. H. (1982) *J. Magn. Reson. 48*, 234–264.
Mayer, A., Ogawa, S., Shuylman, R. G., Yamane, T., Cavaleiro, J. A., Rocha-Gonsalves, A. M. d'A., Kenner, G. W., & Smith, K. M. (1974) *J. Mol. Biol. 86*, 749–756.
Morrow, J. S., & Gurd, F. R. N. (1975) *CRC Crit. Rev. Biochem. 3*, 221–287.
Pande, U., La Mar, G. N., Lecomte, J. T. J., Ascoli, F., Brunori, M., Smith, K. M., Pandey, R. K., Parish, D. W., & Thanabal, V. (1986) *Biochemistry 25*, 5638–5646.
Peyton, D. H., La Mar, G. N., & Gersonde, K. (1988) *Biochim. Biophys. Acta 954*, 82–94.
Ramaprasad, S., Johnson, R. D., & La Mar, G. N. (1984) *J. Am. Chem. Soc. 106*, 5330–5335.
Sandström, J. (1982) *Dynamic NMR Spectroscopy*, Academic Press, New York.
Satterlee, J. D. (1986) *Annu. Rep. NMR Spectrosc. 17*, 79–178.
Satterlee, J. D., Erman, J. E., La Mar, G. N., Smith, K. M., & Langry, K. C. (1983) *J. Am. Chem. Soc. 105*, 2099–2104.
Senn, H., Keller, R. M., & Wüthrich, K. (1980) *Biochem. Biophys. Res. Commun. 92*, 1362–1369.
Shulman, R. G., Glarum, S. H., & Karplus, M. (1971) *J. Mol. Biol. 57*, 93–115.
Takano, T. (1977) *J. Mol. Biol. 110*, 537–568.
Tentori, L., Vivaldi, G., Carla, S., Marinucci, M., Massa, A., Antonini, E., & Brunori, M. (1973) *Int. J. Pept. Protein Res. 5*, 187–200.
Thanabal, V., de Ropp, J. S., & La Mar, G. N. (1987) *J. Am. Chem. Soc. 109*, 265–272.
Traylor, T. G., & Berzinis, A. P. (1980) *J. Am. Chem. Soc. 102*, 2844–2846.
Wittenberg, B. A., Brunori, M., Antonini, E., Wittenberg, J. B., & Wyman, J. (1965) *Arch. Biochem. Biophys. 111*, 576–579.

^{31}P NMR Magnetization-Transfer Measurements of ATP Turnover during Steady-State Isometric Muscle Contraction in the Rat Hind Limb in Vivo†

Kevin M. Brindle,* Martin J. Blackledge, R. A. John Challiss,‡ and George K. Radda
Department of Biochemistry, University of Oxford, South Parks Road, Oxford OX1 3QU, United Kingdom
Received December 2, 1988; Revised Manuscript Received February 7, 1989

ABSTRACT: ^{31}P NMR magnetization-transfer measurements have been used to measure the flux between ATP and inorganic phosphate during steady-state isometric muscle contraction in the rat hind limb in vivo. Steady-state contraction was obtained by supramaximal sciatic nerve stimulation. Increasing the stimulation pulse width from 10 to 90 ms, at a pulse frequency of 1 Hz, or increasing the frequency of a 10-ms pulse from 0.5 to 2 Hz resulted in an increase in the flux which was an approximately linear function of the increase in the tension–time integral. The flux showed an approximately linear dependence on the calculated free cytosolic ADP concentration up to an ADP concentration of about 90 μM. The data are consistent with control of mitochondrial ATP synthesis by the cytosolic ADP concentration and indicate that the apparent K_m of the mitochondria for ADP is at least 30 μM.

^{31}P NMR has been used extensively to monitor the concentrations of ATP, ADP, P_i, phosphocreatine, and H^+ in skeletal muscle in vivo and the changes in these concentrations in response to muscle contraction (Radda, 1986). The energy cost of contraction, in terms of ATP utilization, can be determined by gating the NMR acquisition to various time points after the initiation of tetanic contraction (Shoubridge & Radda, 1987). Since the ATP concentration during a tetanus is maintained at the expense of phosphocreatine, the rate of ATP utilization can be determined from the equal rates of phosphocreatine breakdown or P_i production. In this experiment, the rate of ATP utilization is determined by monitoring the transient response of the muscle as it is stimulated to contract from rest. A powerful feature of the NMR experiment, however, is the facility, using magnetization-transfer

† This work was supported by the Medical Research Council of Great Britain. K.M.B. was the recipient of a University Research fellowship from the Royal Society, and R.A.J.C. was financially supported by the Wellcome Trust.
‡ Present address: Department of Pharmacology and Therapeutics, Medical Sciences Building, University of Leicester, University Rd., Leicester LE1 9HN, U.K.

0006-2960/89/0428-4887$01.50/0